Chapter 2

Detecting *In Vivo* Free Radicals in Various Disease Models

Rheal A. Towner and Nataliya Smith

Additional information is available at the end of the chapter

http://dx.doi.org/10.5772/intechopen.74106

Abstract

In vivo free radical imaging in pre-clinical models of disease is now possible. Free radicals have traditionally been characterized by ESR or EPR spin trapping spectroscopy. The disadvantage of the ESR/EPR approach is that spin adducts are short-lived due to biological reductive and/or oxidative processes. Immuno-spin trapping (IST) involves the use of an antibody that recognizes macromolecular DMPO-spin adducts (anti-DMPO antibody), regardless of the oxidative/reductive state of trapped radical adducts. The IST approach has been extended to an *in vivo* application that combines IST with molecular magnetic resonance imaging (mMRI). This combined IST-mMRI approach involves the use of a spin trapping agent, DMPO, to trap free radicals in disease models, and administration of a mMRI probe, an anti-DMPO probe, that combines an antibody against DMPO-radical adducts and a MRI contrast agent, resulting in targeted free radical adduct detection. The combined IST-mMRI approach has been used in several rodent disease models, including diabetes, ALS, gliomas, and septic encephalopathy. The advantage of this approach is that heterogeneous levels of trapped free radicals can be detected directly *in vivo* and *in situ* to pin-point where free radicals are formed in different tissues. The approach can also be used to assess therapeutic agents that are either free radical scavengers or generate free radicals. The focus of this review will be on the different applications that have been studied, advantages and limitations, and future directions.

Keywords: immuno-spin trapping (IST), molecular magnetic resonance imaging (mMRI), targeted free radical imaging, *in vivo*, diabetes, amyotrophic lateral sclerosis (ALS), glioma, septic encephalopathy, mice, rats

1. Introduction

1.1. Free radicals in various diseases

Reactive oxygen and nitrogen species (RONS) lead to structural and functional modifications of cellular proteins and lipids, resulting in cellular dysfunction, such as impaired energy metabolism, altered cell signaling and cell cycle control, impaired cell transport processes and dysfunctional biological activities, immune activation, and inflammation [1]. RONS can be involved in several disease processes as causative agents or result as an effect of the pathogenesis. It is well known that free radicals play a role in the pathogenesis associated with various diseases such as diabetes, septic encephalopathy, neurodegenerative diseases, and cancers, to mention a few.

Nutritional stress, that for instance may result from excessive high-fat and/or carbohydrates, can promote oxidative stress, subsequently forming lipid peroxidation products, protein carbonylation, as well as decreased antioxidant levels [1]. Chronic oxidative stress and inflammation, both associated with obesity, can lead to insulin resistance, dysregulated metabolic pathways, diabetes and cardiovascular diseases, via impaired signaling and metabolism that result in insulin secretion dysfunction, insulin action, and immune responses [1]. In type 1 diabetes mellitus, RONS released from phagocytes may damage adjacent cells, which can lead to excessive inflammation and an autoimmune attack against pancreatic islet β-cells, and contribute to a rapid progression of pathogenesis [1]. Immune system-associated enzymes (such as NADPH oxidase) can trigger the formation of reactive oxygen species (ROS) [1]. Excessive glucose and lipid levels, endocrine factors and numerous pro-inflammatory cytokines are known to activate NADPH oxidase [1]. Pro-inflammatory cytokines can also upregulate nitric oxide synthase 2 (NOS2), producing excessive nitric oxide, which can subsequently lead to the formation of peroxynitrite, and lead to further oxidative stress [1]. In Type 2 diabetes mellitus, excessive RONS production from chronic hyperglycemia increases oxidative stress in tissues that exacerbate the disease, such as pancreatic islets, muscle, adipose and hepatic, as well as influences secondary diabetic complications, including nephropathy, vascular disease and retinopathy, leading to oxidized lipids and proteins [1, 2].

Sepsis-associated encephalopathy pathophysiology is still poorly understood, but a number of mechanisms-of-action (MOA) have been proposed, including mitochondrial and vascular dysfunction, oxidative damage, neurotransmission disturbances, inflammation, and cellular death [3, 4]. Oxidative stress is a central MOA of acute brain damage [3]. Systemic inflammation induces mitochondrial dysfunction, which is involved in both apoptotic and necrotic cell death pathways, and increased glucose uptake by brain tissues, which results in the diversion of glucose to the pentose phosphate pathway that may contribute to oxidative stress by producing excessive superoxide radicals via NADPH oxidase [3, 4]. In addition, microglia activation results in the secretion of nitric oxide, ROS (reactive oxygen species) and matrix metalloproteinases (MMPs) that can all contribute to blood-brain barrier (BBB) and neuronal damage [3]. Regarding brain dysfunction in sepsis, it is thought that RONS, generated during a systemic inflammatory response, triggers lipid peroxidation due to a decreased antioxidant activity [4]. Free radical-induced structural membrane damage also induces neuro-inflammation [4].

The formation of excessive superoxide radicals also depletes ambient nitric oxide in the cerebrovascular bed, forming peroxynitrite, which irreversibly inhibits the mitochondrial electron transport chain, resulting in an increase in mitochondrial release of free radicals, and leads to mitochondrial dysfunction and neuronal bioenergetics failure [4]. Additionally, free radicals trigger apoptosis via altering intracellular calcium homeostasis in brain regions such as the cerebral cortex and hippocampus, further exacerbating local inflammatory responses further [4].

Oxidative stress has been proposed as a contributory factor in the pathogenesis of several neurodegenerative diseases [5]. For instance, in familial ALS (amyotrophic lateral sclerosis) (accounting for 5–10% of ALS cases) there is a mutation in superoxide dismutase 1 (SOD1) which results in dysfunctional superoxide radical clearance, leading to increased oxidative stress [5]. NADPH oxidases have emerged as possible drug targets for the treatment of neurodegeneration, due to their role in generating oxidants and also regulating microglia activation [6].

In cancer cells, RONS accumulation can result in damaging DNA, directly through an increase in cellular mutations and/or increase in oncogenic phenotypes, or indirectly by acting as secondary messengers intracellular signaling cascades [7]. It is thought that impaired cellular repair mechanisms induced by RONS oxidative stress on DNA can lead to cell injury and subsequently to genomic instability, mutagenesis and tumorigenesis [7]. It is also known that ROS can promote cell proliferation activating growth-related signaling pathways [7]. ROS may be involved in the multistep oncogenesis process at various different phases related to tumor initiation and progression, ROS-related mechanisms during tumor promotion, maintenance of the transformed state through extracellular superoxide radical formation by NADPH oxidase 1, and resistance to oxidative stress signals through membrane-associated catalase expression [7].

1.2. Spin trapping and ESR/EPR spectroscopy

For over half a century, free radicals were characterized by electron spin resonance (ESR) or electron paramagnetic resonance (EPR) spectroscopy coupled with spin trapping. Nitrone spin traps (*N*-oxides of imines), such as PBN (*α*-phenyl-*tert*-butyl nitrone), DMPO (5,5-dimethyl-pyrroline-*N*-oxide) or 4-POBN (*α*(4-pyridyl-1-oxide)-N-tert-butyl nitrone), are the most commonly used for biological systems [8–18], and have been administered *in vivo* in various pre-clinical disease models [19–22] for several decades.

The disadvantage of the ESR/EPR approach is that the spin adducts (spin trapping agent — free radical adducts or aminoxyls) are short-lived due to reductive and/or oxidative processes in biological systems [8, 9] (see **Figure 1**).

1.3. Immuno-spin trapping (IST)

Mason *et al*. developed an antibody that recognizes macromolecular DMPO spin adducts, regardless of the oxidative/reductive state of the trapped radical adducts, and called the methodology immuno-spin trapping (IST) [23–28] (see **Figure 2** for an illustrative description), that has been applied in over 80 publications. The anti-DMPO antibody is attached to a fluorescent dye, allowing the *in vitro* or *ex vivo* detection of trapped DMPO-radical adducts,

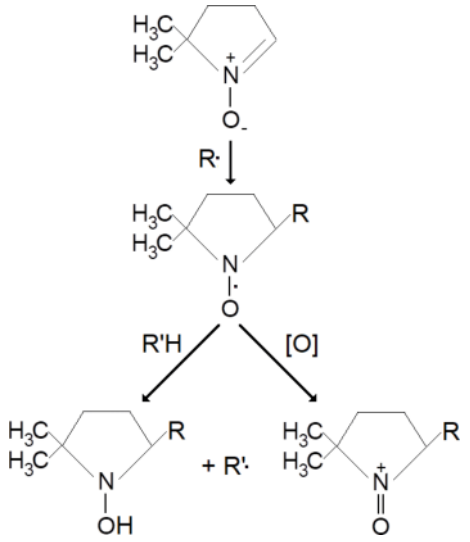

Figure 1. Spin trapping agents (nitrones) can be used to trap free radical compounds (R•) to form a spin adduct (nitroxide or aminoxyl), which are detected by EPR spectroscopy. However, in biological systems spin adducts can be either reduced (R'H) or oxidized ([O]). Reduced or oxidized spin adducts are EPR silent.

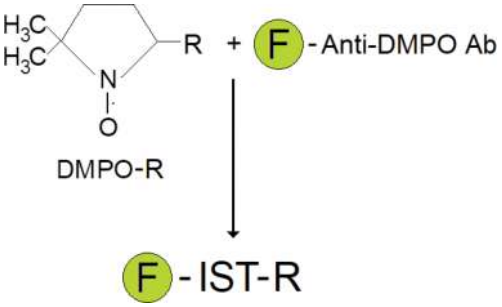

Figure 2. Immuno-spin trapping (IST) involves tagging a fluorescent-labeled-anti-DMPO antibody to DMPO-spin adducts (either as the free radical (aminoxyl), reduced or oxidized products, i.e. regardless of whether they are EPR detectable or not). The "F" designates a fluorescent dye.

either as the free radical (aminoxyl), reduced or oxidized products, with fluorescence microscopy, regardless of whether they are EPR detectable or not.

1.4. Combined IST and molecular MRI (mMRI) detection of *in vivo* and *in situ* free radicals

Towner *et al*. extended the fluorescence *in vitro/ex vivo* approach to an *in vivo* approach that involves the use of immuno-spin trapping (IST) in conjunction with targeted molecular magnetic resonance imaging (mMRI), currently published in six publications [29–34]. This

involves the use of a spin trapping agent, DMPO, which is used to trap free radicals in an oxidative stress-related disease model, and administration of a mMRI probe, called an anti-DMPO probe (see **Figure 3**), that combines an antibody against DMPO-radical adducts and a MRI contrast agent, resulting in targeted free radical adduct mMRI (see **Figure 4** for methodology scheme). The contrast agent used in the Towner approach includes an albumin-Gd-DTPA (gadolinium diethylene tri-amine penta-acetic acid)-biotin construct, where the anti-DMPO antibody is covalently linked to the cysteine residues of albumin, forming an anti-DMPO-adduct antibody-albumin-Gd-DTPA-biotin entity. The Gd-DTPA moiety acts as the MRI signaling component, which will increase MRI signal intensity (SI) in a T_1-weighted morphological MR imaging sequence, and decrease T_1 relaxation in a T_1 map image. Both of these parameters, MRI SI or T_1 relaxation) can be used to assess the presence of the anti-DMPO probe. The biotin moiety can be used for *ex vivo* validation of the presence of the anti-DMPO probe in tissues, by using a streptavidin-fluorescent dye (e.g. Cy3) or streptavidin-HRP (horse radish peroxidase) to tag the biotin in the anti-DMPO probe.

1.5. Other approaches used to detect *in vivo* and *in situ* free radicals in animal models and cells

It is well known that intensity-based fluorescent methods (particularly 2′,7′-dicholorofluorescin [DCFH]) for ROS (includes the non-radical hydrogen peroxide) detection/quantification are sensitive and readily used, however, these agents lack the specificity for ROS or reactive nitrogen species (RNS), and often produce artifacts resulting in false-positive signals [35, 36]. An interesting recent study by Liu et al. used a new fluorescent probe, MPT-Cy2, which can be used to detect endogenous *in vivo* hydroxyl radicals in cells and zebrafish [37]. MPT-Cy2 becomes a fluorescent product, OMPT-Cy2, when it binds hydroxyl radicals [37]. In a similar fashion, Hu et al. reported on a fluorescent probe, HKSOX-1, for the imaging and

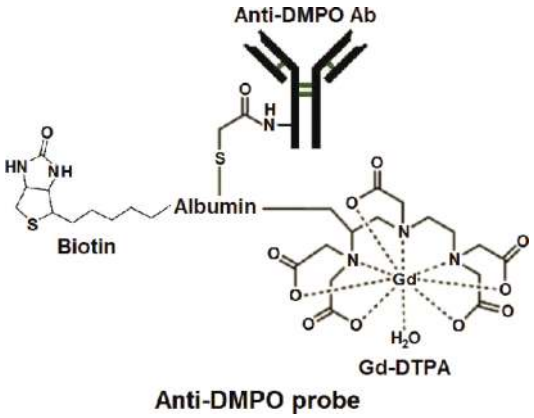

Figure 3. Illustration of the anti-DMPO probe, consisting of an albumin link that binds a MRI contrast agent, Gd-DTPA (for detection by MRI), the anti-DMPO antibody (Ab) (that binds to DMPO-free radical adducts), and biotin (that can be used for ex vivo fluorescence microscopic imaging). Modified from Gomez-Mejiba et al. [28].

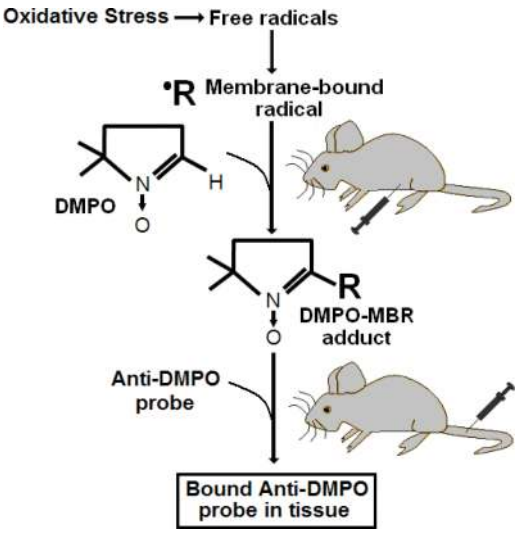

Figure 4. Combined IST and free radical-targeted molecular MRI (mMRI) approach. Initially mice are administered DMPO (i.p.) to trap free radicals resulting from an oxidative stress-associated disease or process. Any cell membrane-bound radicals (e.g. oxidized proteins or lipids) can then be detected with the anti-DMPO probe (administered via a tail-vein catheter). Modified from Towner et al. [29].

detection of endogenous *in vivo* superoxide in cells and zebrafish embryos [38]. A fluorescence probe, o-phenylene diamine-Phe-Phe-OH, has also been developed for the detection of nitric oxide (NO), and used in living cells [39]. Another fluorescence probe, LyNP-NO, was used to detect NO in C6 glioma cells [40]. It was also found that single-walled carbon nanotubes have fluorescent properties, and have been used to detect *in vivo* levels of NO, which quenches the fluorescence signal, in mice [41]. However, for most of the fluorescence probes *in vivo* applications will be limited to a depth-of-penetration detection of the fluorescence signal and may only be applicable to small animal models.

Another group, Li et al. used a near infrared (NIR)-light excited luminescence resonance energy transfer based nanoprobe for *in vivo* detection of hydroxyl radicals [42]. NIR fluorescence probes (Hcy-Mito and Hcy-Biot) were also recently used for the *in situ* detection of superoxide anion and hydrogen polysulfides in living cells and in mouse tumor models [43]. Also, a phosphinate-based NIR fluorescence probe, CyR, was recently also used to detect superoxide radical anion *in vivo* within zebrafish [44]. NIR-fluorescent single-walled carbon nanotubes have also been used to detect *in vivo* NO levels in mice [45]. It should be pointed out, however, that there is ESR spectroscopy evidence for *in vivo* formation of free radicals in the tissues (lungs, heart and liver) of mice exposed to single-walled carbon nanotubes with no oxidative stress [46].

Rayner et al. used a reversible pro-fluorescent probe containing a redox sensitive nitroxide moiety (methyl ester tetraethylrhodamine nitroxide, ME-TRN) for the *in vivo* detection of retinal oxidative status within rat retina following acute ischemia-reperfusion injury [47].

Another interesting approach using nitrone functionalized gold nanoparticles (Au@EMPO, EMPO = 2-(ethoxycarbonyl)-2-methyl-3,4-dihydr-2H-pyrrole 1-oxide)) to trap hydroxyl radicals was demonstrated by Du et al. [48] and may be potentially important for pre-clinical *in vivo* applications in combination with micro-computed tomography (CT).

Recent studies by Berkowitz et al. have used quench-assisted (Quest) $1/T_1$ MRI to measure oxidative stress changes in rodent models [49, 50]. Quest MRI detected pathologic free radical production in MnSOD (manganese superoxide dismutase) knockout mouse retinas with laminar resolution *in vivo*, where in particular dark-adapted RPE-specific MnSOD knockout mice had elevated $1/T_1$ values in the outer retina, compared to relevant controls [49] The Quest MRI technique was also used to report on high levels of free radicals in the hippocampus region in mouse models for neurological diseases such as Alzheimer's disease and Angelman syndrome [50]. However, it should be noted that paramagnetic oxygen [49–51] and hydrogen peroxide [50, 51] can also provide a dominant $1/T_1$ contrast effect, which could complicate the interpretation of the presence of free radicals. In addition, temperature and pH also can influence the rates of proton exchange which will also affect $1/T_1$ contrast [52, 53]. Nonetheless, Quest MRI is an interesting approach that provides information on total free radical burden, somewhat similar to the combined IST and mMRI approach, but without the use of a MRI contrast agent [49, 50].

Endogenous reactive oxygen species (ROS) contrast MRI was also recently used by Tain et al. to detect ROS (measured as a reduction in T_1) in rotenone-treated mouse brains [51]. Another study by Eto et al. used *in vivo* nuclear polarization MRI (DNP-MRI) with nitroxyl radicals (carbamoyl-PROXYL (cell permeable) and carboxy-PROXYL (cell impermeable)) to assess the redox status (measured as an increase in image intensity) in the skeletal muscle of mice that had an acute local inflammation (induced with i.m. injection of bupivacaine) [54]. The signal decay of carbamoyl-PROXYL in bupivacaine-exposed mice was confirmed by *in vivo* L-band EPR spectroscopy [54]. The nitroxyl radical probes, are paramagnetic which broaden the MRI signal, bind free radicals, and thus results in an increase in MRI signal intensity [55]. Another group used DNP-MRI to visualize endogenous free radical intermediates of FMNH (flavin mononucleotide-hydrogen) and FADH (flavin adenine dinucleotide-hydrogen) *in* vitro [56], which could potentially be detected *in vivo* in the future. DNP-MRI, also used for PEDRI (proton electron double-resonance imaging) or OMRI (Overhauser enhanced magnetic resonance imaging), is a relatively new imaging approach for detecting free radical species *in vivo* [57, 58]. Yamamoto et al. recently developed a combined PET (positron emission tomography)/OMRI system to detect radionucleotide and nitroxyl radical probes for small animal imaging [59].

1.6. Overall scope

The focus of this review is on *in vivo* and *in situ* IST-mMRI applications in different experimental oxidative stress-associated animal disease models that have been studied, advantages and limitations of the technique, and future directions in further applications, improvements on the methodology that can be made, and subsequent free radical identification approaches.

2. *In vivo* and *In situ* targeted free radical detection: various models

The combined IST-mMRI approach has been used in several *in vivo* disease models, including multi-tissue assessment in diabetic mice [29] (see **Figure 5**) with further assessment of cardiomyopathy [30] (see **Figure 6**), and in neurological applications, such as rodent models septic encephalopathy [31] (see **Figure 8**), for amyotrophic lateral sclerosis (ALS) [32] (see **Figure 7**), and gliomas [33], to target *in vivo* and *in situ* free radical detection.

2.1. Diabetes

The initial proof-of-concept combined IST and mMRI approach to detect *in vivo* free radicals was assessed in a STZ (streptozotocin)-induced diabetes model in mice. From this study, all major organs excluding the heart, such as the lungs, liver and kidneys, were assessed regarding levels of trapped *in vivo* and *in situ* DMPO-radical adducts [29]. **Figure 5** depicts the data obtained in the liver of diabetic (STZ-induced) and non-diabetic mice (wild-type

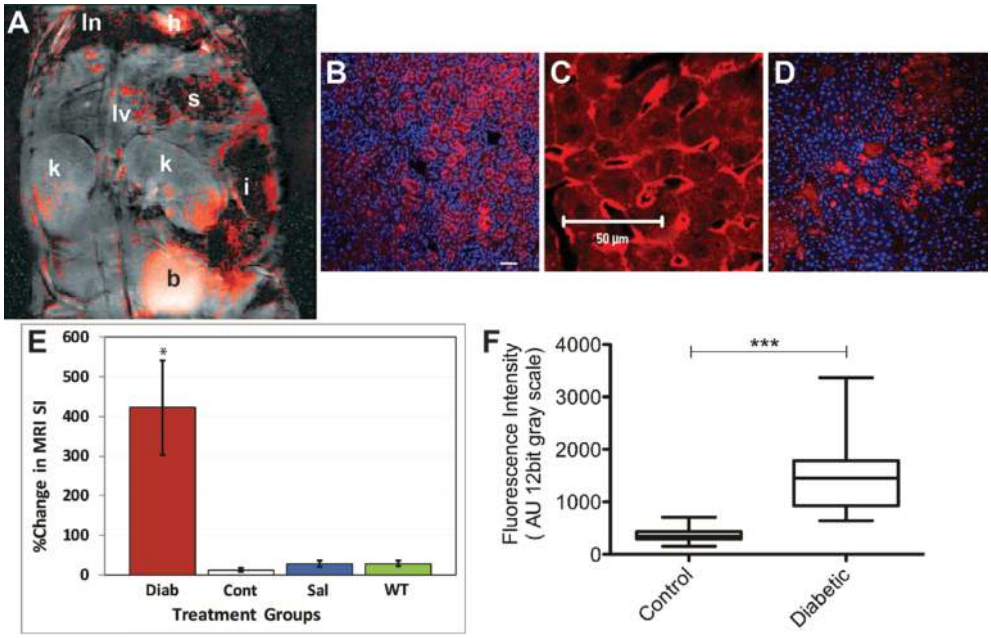

Figure 5. Combined IST and free radical-targeted mMRI in a STZ-induced mouse diabetic model. (A) *In vivo* anti-DMPO probe distribution map (based on MRI signal intensity (SI) change). Anatomical assignments: ln = lung, h = heart, s = stomach, lv = liver, k = kidney, i = intestine, and b = bladder. (B) Stretavidin-Cy3 biotin-tagged *ex vivo* liver image in Diab mice. (C) iNOS immunohistochemistry (IHC) from the liver of a diabetic mouse. (D) Fluorescence intensity of iNOS IHC in non-diabetic (control) and diabetic mouse livers. N = 5 for each. (E) Percent (%) change in MRI SI in diabetic mice administered DMPO + anti-DMPO probe (Diab), DMPO + a non-specific IgG contrast agent (Cont), saline + anti-DMPO probe (Sal), and wild-type non-diabetic mice administered DMPO + anti-DMPO probe. N = 5 for each group. (F) Fluorescent-IST image of the liver of a diabetic mouse. Modified from Towner et al. [29].

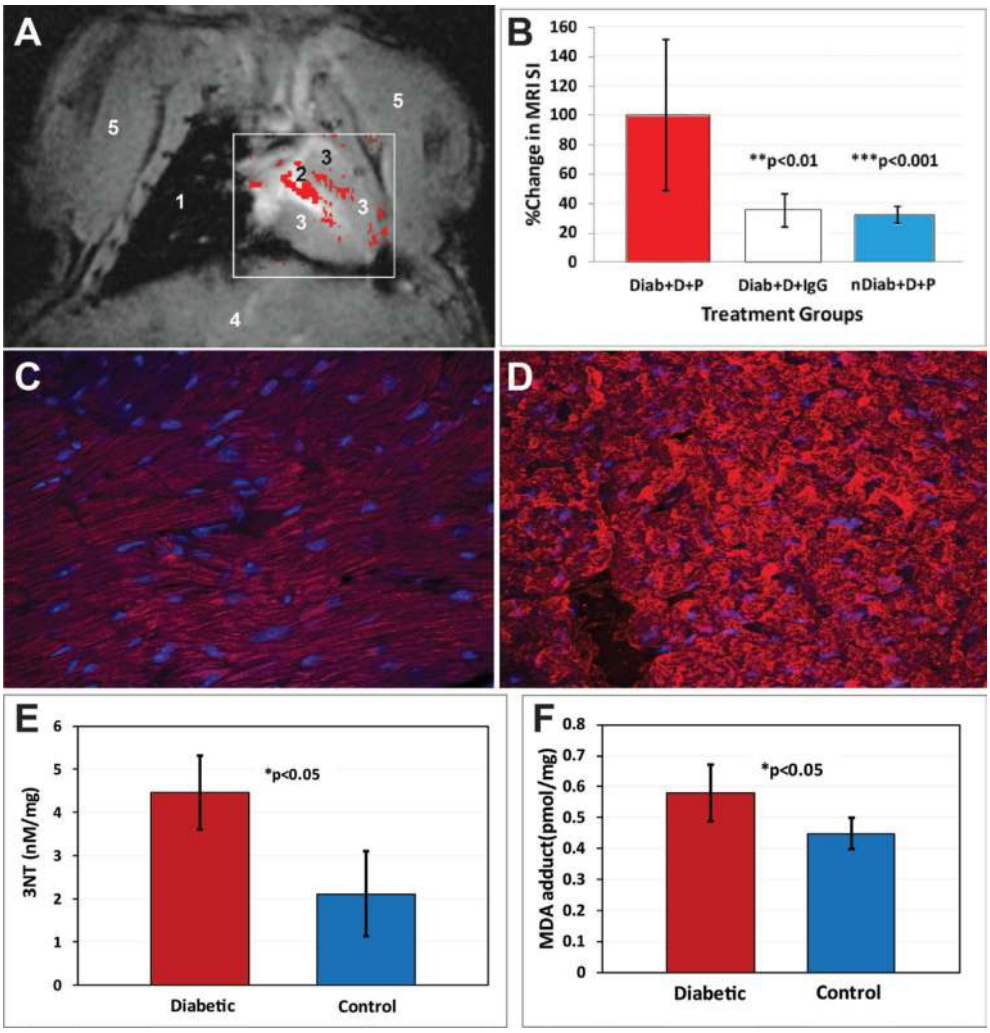

Figure 6. Combined IST and free radical-targeted mMRI in a STZ-induced mouse diabetic heart. (A) MR image of a mouse heart with an *in vivo* anti-DMPO probe cardiac map overlay (based on MRI SI change). Anatomical assignments: 1 = lung, 2 = left ventricle chamber, 3 = cardiac muscle, 4 = liver, and 5 = thoracic muscle. (B) Percent (%) change in MRI SI in diabetic mouse hearts after administered DMPO + anti-DMPO probe (Diab+D + P), DMPO + a non-specific IgG contrast agent (Diab+D + IgG), and non-diabetic mice administered DMPO + anti-DMPO probe (nDiab+D + P). N = 5 for each group. (C) Stretavidin-Cy3 biotin-tagged *ex vivo* cardiac image in Diab mice. (D) Fluorescent-IST image of the heart of a diabetic mouse. (E) 3-Nitrotyrosine (3-NT) adducts and (F) malondialdehyde (MDA) ELISAs from the hearts of diabetic and non-diabetic mice. N = 5 for each. Modified from Towner et al. [30].

mice not administered STZ), and appropriate controls (e.g. diabetic mice given saline rather than DMPO plus the anti-DMPO probe — spin trap control; or a diabetic mouse administered DMPO, but given a non-specific IgG contrast agent [IgG-albumin-Gd-DTPA-biotin] instead

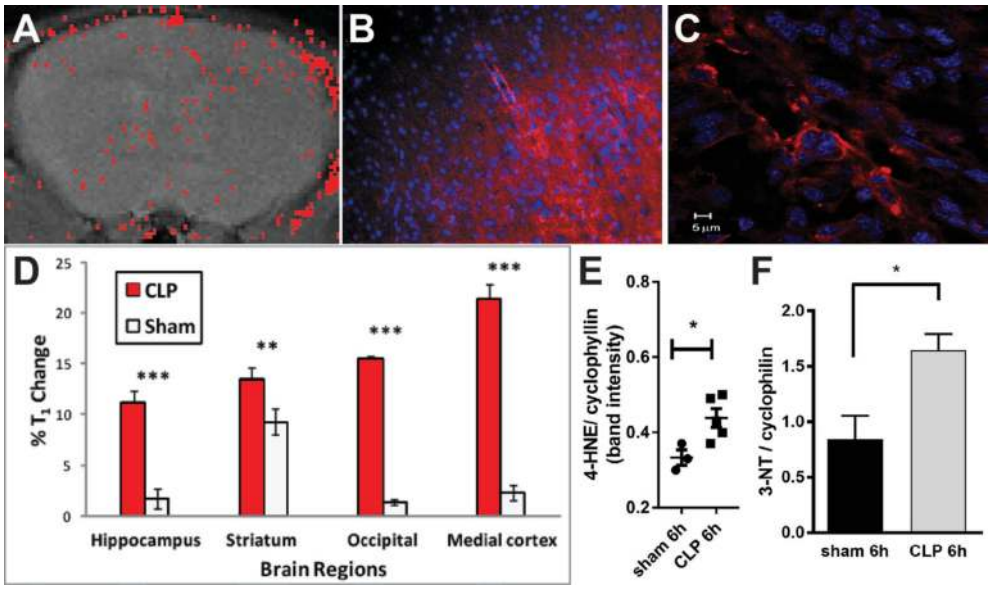

Figure 7. Combined IST and free radical-targeted mMRI in a septic encephalopathy CLP-induced mouse model. (A) *In vivo* anti-DMPO probe brain map of a septic mouse (based on MRI SI change). (B) Stretavidin-Cy3 biotin-tagged *ex vivo* septic brain image. (C) Fluorescent-IST image of the septic brain of a mouse. (D) Percent (%) T1 relaxation change in septic and sham mice administered DMPO + anti-DMPO probe in different brain regions (hippocampus, striatum, occipital lobe, and medial cortex). N = 5 for each group. (E) 4-Hydroxynonenal (4HNE) levels from western blots of brains of septic and non-septic mice. (F) 3-Nitro-tyrosine (3-NT) levels from western blots of brains of septic and non-septic mice. N = 5 for each. Modified from Towner et al. [31].

of the anti-DMPO probe). (**Figure 5**) Diabetic mice that were administered DMPO and the anti-DMPO probe, had significantly higher levels of the anti-DMPO probe (detected by an increase in percent (%) change in MRI SI), than non-diabetic mice or diabetic mouse controls, in their lungs, kidneys and livers (see **Figure 5A** for overall distribution of the anti-DMPO probe in a horizontal image; and **Figure 5E** for quantitative liver data). A post-contrast image minus a pre-contrast image was obtained, and the gray-scale image was false-colored red, and overlaid on top of the morphological image. Non-specific biodistribution of the anti-DMPO was also found in the stomach, intestines, and bladder (**Figure 5A**). From kinetics assessment, it was found that the anti-DMPO probe persisted in certain tissues (e.g. lungs, liver and kidneys) for over 3 hours. Verification of the presence of the anti-DMPO probe in ex vivo tissues was done by using streptavidin-Cy3 which bound to the biotin moiety of the anti-DMPO probe (see **Figure 5B** for example in liver tissue). It was also confirmed that DMPO-radical adducts were formed by using a fluorescent-anti-DMPO antibody (IST approach) in diabetic (see **Figure 5C**) and non-diabetic mouse livers. In addition, inducible nitric oxide synthase (iNOS) levels were assessed in the livers of diabetic and non-diabetic mice (see **Figure 5D** for immunohistochemistry (IHC) detection of iNOS in a diabetic mouse liver; and **Figure 5F** for quantitative levels of iNOS in diabetic and non-diabetic mouse livers) as an additional marker of oxidative stress. This was the first *in vivo* study to demonstrate that diabetic mice had elevated *in situ* free radical levels in organs/tissues such as the lungs, liver and kidneys.

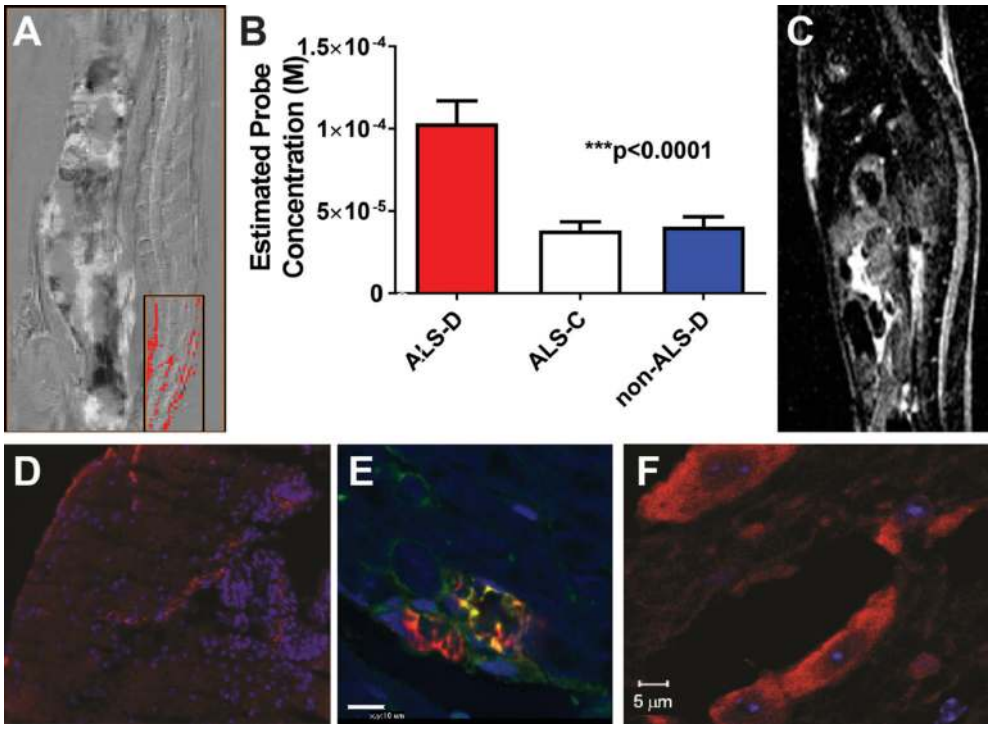

Figure 8. Combined IST and free radical-targeted mMRI in an ALS mouse model. (A) *In vivo* anti-DMPO probe map (based on MRI signal intensity (SI) change). (B) DMPO probe concentration in ALS mice administered DMPO + anti-DMPO probe (ALS-D), DMPO + non-specific IgG contrast agent (ALS-C), and wild-type non-ALS mice administered DMPO + anti-DMPO probe (non-ALS-D). N = 5 for each group. (C) Diffusion-weighted image of an ALS mouse with increased apparent diffusion coefficient (ADC) in lumbar region (outlined). (D) Stretavidin-Cy3 biotin-tagged *ex vivo* spinal cord in ALS-D. (E) Co-localized DMPO probe (red) and neuronal marker (green) fluorescence image in mouse spinal cord. (F) Fluorescent-IST image of the spinal cord of an ALS mouse. Modified from Towner et al. [32].

At a later stage it was found that the cardiac muscle in diabetic mice also retained the anti-DMPO probe [30] (see **Figure 6**). A morphological MR image of a mouse heart is shown in **Figure 6A**. The post-contrast minus pre-contrast image in a diabetic mouse with false coloration is shown in **Figure 6A**, overlaid on top of a horizontal morphological image of the heart.

Significantly higher quantitative levels of the anti-DMPO probe in diabetic (Diab) mice administered DMPO (D) and the anti-DMPO probe (P) were found when compared to diabetic (administered the isotype IgG contrast agent instead of the anti-DMPO probe) and non-diabetic (non-STZ exposed WT mice administered DMPO and the anti-DMPO probe) controls (see **Figure 6B**). Confirmation of the presence of the anti-DMPO probe in cardiac muscle of a diabetic mouse is shown in **Figure 6C**. Verification of the presence of DMPO-radical adducts is shown in **Figure 6D**, where a fluorescent-labeled anti-DMPO antibody was used. In the diabetic cardiomyopathy study, it was also established that diabetic mice had significantly higher levels of 3-nitrotyrosine (3-NT) (oxidized protein marker) (**Figure 6E**) and malondi aldehyde (MDA) adducts (oxidized lipid marker) (**Figure 6F**) in cardiac muscle, when compared

to non-diabetic mice. This was the first *in vivo* study to demonstrate increased *in situ* free radical levels in diabetic cardiomyopathy. The correlation with oxidized lipids and proteins was done, as it is suspected that the combined IST and mMRI approach primarily reports on macromolecular free radicals that are cell-membrane bound. Mason et al. have previously reported on the application of IST to trap oxidized proteins [23–25]. As both an increase in oxidized lipids and proteins were detected in diabetic cardiac muscle via ELISA, it is possible that the combined IST and mMRI method detects both oxidized lipids as well as proteins. Further verification would require a mass spectrometry approach to confirm this assumption.

2.2. Septic encephalopathy

It was then decided to assess the combined IST and mMRI free radical-targeted approach in other disease models, such as septic encephalopathy. Mice with septic encephalopathy (induced by cecal ligation and puncture (CLP)) were also found to have higher levels of trapped DMPO-radical adducts compared to sham animals (abdominal incision without CLP and sutured) [31] (**Figure 7**). **Figure 7A** depicts a MRI SI difference image (false-colored red) overlaid on top of a morphological image of the brain region of a septic mouse. Confirmation of the presence of the anti-DMPO in the cortical brain tissue of a septic mouse is shown in **Figure 7B**, and verification of DMPO-radical adducts in a septic mouse brain is depicted in **Figure 7C**. The distribution of the anti-DMPO probe is dispersed throughout the brain, and was found to be significantly higher in septic mice vs. sham animals in the hippocampus, striatum, occipital lobe and medial cortex regions of the brain (**Figure 7D**), as measured by a % change (overall decrease in T_1 relaxation). Oxidized lipid levels (measured from Western blots for 4-hydroxynonenal (4-HNE) (**Figure 7E**) and oxidized protein levels (measured from Western blots for 3-NT) (**Figure 7F**) were found to be significantly higher in septic mice (CLP) after 6 hours, compared to sham controls. This study also indicates that both oxidized lipids and proteins may play a role in the free radical-associated pathology of ALS. This is the first reported *in vivo* detection of elevated *in situ* free radicals in a mouse model for septic encephalopathy.

2.3. Amyotrophic lateral sclerosis (ALS)

The combined IST and mMRI approach for detecting *in vivo* free radicals was extended to other neurological disorders, such as ALS. High levels of trapped DMPO-radical adducts were also found in a transgenic mouse model for ALS (superoxide dismutase (SOD) mutation) [32] (see **Figure 8**). As SOD1 plays an important role in $O_2^{-\bullet}$ clearance, the loss of SOD1 can lead to increased levels of free radicals [5]. A pre-contrast minus post-contrast difference sagittal image is shown in **Figure 8A** for an ALS mouse, with false coloration depicted in the lumbar region of the spinal cord. From T_1 relaxation values the estimated anti-DMPO probe concentration can be obtained, and it was found that ALS mice administered DMPO and the anti-DMPO probe (ALS-D) had significantly higher levels of the anti-DMPO probe, compared to ALS (administered the IgG contrast agent instead of the anti-DMPO probe) and non-ALS (administered both DMPO and the anti-DMPO probe) controls (see **Figure 8B**). A diffusion-weighted image is shown in **Figure 8C** depicting a high signal intensity in the lumbar region of the spinal cord. *Ex vivo* detection of the anti-DMPO probe in the lumbar region of the spinal cord of an ALS mouse is shown in **Figure 8D**. **Figure 8E** illustrates that a neuronal marker

(NrCAM) (green) co-localizes with the location of the anti-DMPO probe (red) in some regions (yellow). Confirmation of DMPO-radical adducts is depicted in **Figure 8F**. This is the first direct *in vivo* detection of elevated *in situ* free radicals in the lumbar region of ALS-like mice.

2.4. Gliomas

Lastly, the combined IST and mMRI *in vivo* free radical detection method was applied to assess glioma models, both for untreated and anti-cancer agent treated tumors. It was initially demonstrated that free radicals can be detected in a GL261 mouse glioma model [33]. The DMPO-trapped radicals were found to be heterogeneously distributed primarily in the tumor core region, possibly associated with increased cell proliferation [33]. In addition to confirming the presence of the anti-DMPO probe in glioma tumor tissue and detection of anti-DMPO trapped radicals, it was also possible to demonstrate that GL261 gliomas had elevated levels of MDA protein adducts and 3-NT, compared to normal mouse brain tissue [33].

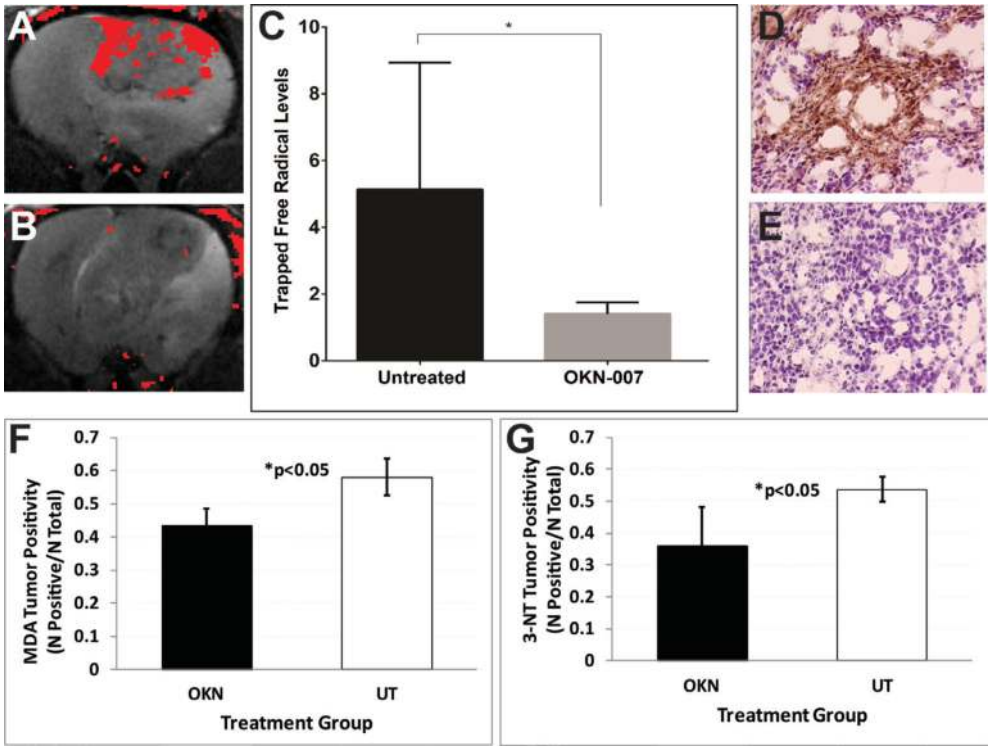

Figure 9. Combined IST and free radical-targeted mMRI in a F98 rat glioma model. *In vivo* anti-DMPO probe brain maps of (A) untreated (UT) and (B) OKN-007-treated rat F98 tumors (based on MRI SI change). (C) Trapped free radical levels (% change in MRI SI) in UT and OKN-007-treated F98 gliomas administered DMPO + anti-DMPO probe. N = 5 for each group. Stretavidin-HRP biotin-tagged ex vivo F98 gliomas that were (D) UT or (E) OKN-007-treated. (F) Malondialdehyde (MDA) levels from IHC of F98 tumors of OKN-007-treated or UT rats. (G) 3-Nitrotyrosine (3-NT) levels from IHC of F98 tumors of OKN-007-treated or UT rats. N = 5 for each. Modified from Coutinho de Souza et al. [34].

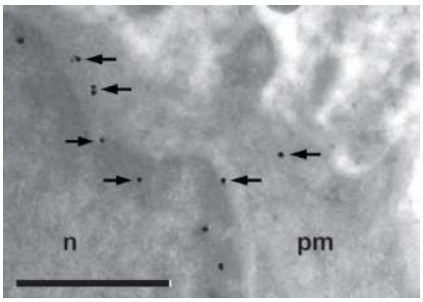

Figure 10. Immuno-electron microscopy detection of the anti-DMPO probe in the plasma membrane/ cytoplasm and cell nuclei in F98 rat gliomas. The biotin moiety of the anti-DMPO probe was targeted with gold-anti-biotin. Gold-anti-biotin colloids were detected within the plasma membrane/cytoplasm (black arrows) and cell nuclei membranes of F98 tumor cells administered the anti-DMPO probe. Scale bar = 1 μm. Magnification = 20,000×. n = nucleus; c = cytoplasm; pm = plasma membrane. Modified from Coutinho de Souza et al. [34].

The combined IST and mMRI approach in glioma models can also be used to assess possible therapeutic agents that are either free radical scavengers or generate free radicals. For example, this approach was used to assess the free radical scavenging ability of an anti-cancer agent, OKN-007, in a rat glioma model [34] (see **Figure 9**). Representative difference images (false-colored red) of an untreated F98 glioma and an OKN-007-treated F98 glioma, overlaid over appropriate morphological images, are shown in **Figure 9A** and **B**, respectively. Quantitative levels of trapped free radical levels (measured from % changes in MRI signal intensities) for untreated and OKN-007-treated F98 gliomas is shown in **Figure 9C**. Significantly lower levels of MDA (**Figure 9F**) and 3-NT (**Figure 9G**) were found for F98 gliomas treated with OKN-007 compared to untreated (UT) tumors. IHC levels for MDA and 3-NT were quantitated in several OKN-007-treated and UT F98 tumor-bearing rats. These results indicate that OKN-007 acts as a free radical scavenger when used as an anti-cancer agent. This is the first time *in vivo* detection of *in situ* free radicals had been reported for an anti-cancer agent with free radical scavenging capability. It was previously demonstrated that OKN-007 can significantly increase animal survival and significantly decrease tumor volumes, when compared to UT animals. The combined IST and mMRI approach can be taken to assess any therapeutic agents that would either increase or decrease free radical levels in different disease models.

Immuno-electron microscopy (IEM) with gold-anti-biotin, targeting the biotin moiety of the anti-DMPO probe, was also used to confirm the *ex vivo* presence of the anti-DMPO probe in the plasma membrane of rat glioma cells following *in vivo* administration [34] (see **Figure 10**). The IEM data is confirmation that the combined IST and mMRI approach is detecting macromolecular membrane-bound (both plasma membrane and possibly nuclear membrane) free radicals.

3. Concluding statements

The novelty of the IST-mMRI approach is that heterogeneous levels of trapped free radicals can be detected directly *in vivo* and *in situ* with high image resolution, and can be used to

pin-point where high levels of free radicals are formed in different heterogeneous regions of specific tissues. It should be noted that MRI has no depth-of-penetration limitation. The current anti-DMPO-albumin-Gd-DTPA-biotin construct allows rapid vascular delivery, and binding to macromolecular DMPO-trapped free radicals in the plasma membrane, as well as *ex vivo* confirmation with microscopy.

This review has discussed all of the current studies that have utilized combined IST and mMRI to detect targeted trapped macromolecular DMPO-radical adducts *in vivo* and *in situ* within various animal models where oxidative stress plays a major role. It was established for all oxidative stress-associated disease models studied thus far, that levels of free radicals were found to be significantly increased in all cases for animals treated with DMPO and the anti-DMPO probe, when compared to controls, including disease controls (e.g. wild-type rodents or shams), non-DMPO controls (i.e. administered saline instead of DMPO), and/or mMRI probe controls (i.e. a non-specific IgG was covalently bound to the albumin of the MRI contrast agent construct instead of the anti-DMPO antibody). An example of assessing an anti-cancer agent with free radical scavenging activity was also presented. The biotin moiety of the anti-DMPO probe also allowed *ex vivo* validation of the presence of trapped DMPO macromolecular adducts in various tissues. IST was also used in all cases to confirm the presence of trapped free radicals with fluorescence or optical (e.g. HRP) microscopy. Finally, IEM was used to confirm the presence of the anti-DMPO probe in plasma and nuclear membranes.

Some of the disadvantages with the methodology include limited access to pre-clinical MRI systems, availability of the anti-DMPO antibody, and further identifying the radical source that is being trapped. For non-neurological studies, this approach can be easily utilized in numerous pathological/toxicological models. However, for neurological studies, the approach will be limited to whether there is BBB permeability, in order to allow the anti-DMPO probe, and possibly DMPO, to access the target tissue.

The IST-mMRI approach can certainly be further applied to study free radicals associated longitudinally in oxidative stress-related disease processes, as well as assess the effect of therapeutic agents that alter free radical levels. Mass spectrometry may need to be used to not only further assess whether the anti-DMPO probe detected in heterogeneous tissue regions are essentially oxidized proteins or oxidized lipids, or a combination of both, before the type of protein or lipid is identified. The current size of the probe may prohibit use in neurological studies with an intact blood-brain barrier (BBB). The development of a smaller nanoparticle-based anti-DMPO probe, which may allow access through an intact BBB, is currently being considered.

Author details

Rheal A. Towner* and Nataliya Smith

*Address all correspondence to: rheal-towner@omrf.org

Advanced Magnetic Resonance Center, Oklahoma Medical Research Foundation, Oklahoma City, OK, USA

References

[1] Newsholme P, Cruzat VF, Keane KN, Carlessi R, Homen de Bittencourt PI Jr. Molecular mechanisms of ROS production and oxidative stress in diabetes. The Biochemical Journal. 2016;**473**:4527-4550

[2] Fakhruddin S, Alanzi W, Jackson KE. Diabetes-induced reactive oxygen species: Mechanism of their generation and role in renal injury. Journal of Diabetes Research. 2017; **2017**:8379327

[3] Bozza FA, D'Avila JC, Ritter C, Sonneville R, Sharshar T, Dal-Pizzol F. Bioenergetics, mitochondrial dysfunction, and oxidative stress in the pathophysiology of septic encephalopathy. Shock. 2013;**39**:10-16

[4] Berg RMG, Moller K, Bailey DM. Neuro-oxidative-nitrosative stress in sepsis. Journal of Cerebral Blood Flow and Metabolism. 2011;**31**:1532-1544

[5] Niedzielska E, Smaga I, Gawlik M, Moniczewski A, Stankowicz P, Pera J, Filip M. Oxidative stress in neurodegenerative diseases. Molecular Neurobiology. 2016;**53**:4094-4125

[6] Sorce S, Stocker R, Seredenina T, Holmdahl R, Aguzzi A, Chio A, Depaulis A, Heitz F, Olosson P, Olsson T, Duveau V, Sanoudou D, Skosgater S, Vlahou A, Wasquel D, Krause KH, Jaquet V. NADPH oxidases as drug targets and biomarkers in neurodegenerative diseases: What is the evidence? Free Radical Biology & Medicine. 2017;**112**:387-396

[7] Rinaldi M, Caffo M, Minutoli L, Marini H, Abbritti RV, Squadrito F, Trichilo V, Valenti A, Barresi V, Altavilla D, Passalacqua M, Caruso G. ROS and brain gliomas: An overview of potential and innovative therapeutic strategies. International Journal of Molecular Sciences. 2016;**17**(6). Pii: E984. DOI: 10.3390/ijms17060984

[8] Towner RA. In: Rhodes C, editor. Chemistry of Spin Trapping, in Toxicology of the Human Environment: The Critical Role of Free Radicals. London: Taylor and Francis; 2000. pp. 7-24

[9] Janzen EG. Spin trapping. Methods in Enzymology. 1984;**104**:188-198

[10] Janzen EG, Stronks HJ, Dubose CM, Poyer JL, McCay PB. Chemistry and biology of spin-trapping radicals associated with halocarbon metabolism in vitro and in vivo. Environmental Health Perspectives. 1985;**64**:151-170

[11] Buettner GR. Spin trapping: ESR parameters of spin adducts. Free Radical Biology & Medicine. 1987;**3**:259-303

[12] McCay PB. Application of ESR spectroscopy in toxicology. Archives of Toxicology. 1987; **60**:133-137

[13] Janzen EG, Poyer JL, Schaefer CF, Downs PE, DuBose CM. Biological spin trapping. II. Toxicity of nitrone spin traps: Dose-ranging in the rat. Journal of Biochemical and Biophysical Methods. 1995;**30**:239-247

[14] Davies MJ, Slater TF. The use of electron-spin-resonance techniques to detect free-radical formation and tissue damage. The Proceedings of the Nutrition Society. 1988;**47**:397-405

[15] Villamena FA, Zweier JL. Detection of reactive oxygen and nitrogen species by EPR spin trapping. Antioxidants & Redox Signaling. 2004;**6**:619-629

[16] Hawkins CL, Davies MJ. Detection and characterisation of radicals in biological materials using EPR methodology. Biochimica et Biophysica Acta. 2014;**1840**:708-721

[17] Barriga-González G, Olea-Azar C, Zuñiga-López MC, Folch-Cano C, Aguilera-Venegas B, Porcal W, González M, Cerecetto H. Spin trapping: An essential tool for the study of diseases caused by oxidative stress. Current Topics in Medicinal Chemistry. 2015; **15**:484-495

[18] Davies MJ. Detection and characterisation of radicals using electron paramagnetic resonance (EPR) spin trapping and related methods. Methods. 2016;**109**:21-31

[19] Mason RP. Assay of *in situ* radicals by electron spin resonance. Methods in Enzymology. 1984;**105**:416-422

[20] Mason RP. In: Rhodes C, editor. *In vivo* Spin Trapping – From Chemistry to Toxicology, in Toxicology of the Human Environment: The Critical Role of Free Radicals. London: Taylor and Francis; 2000. pp. 49-70

[21] Berliner LJ, Khramtsov V, Fujii H, Clanton TL. Unique in vivo applications of spin traps. Free Radical Biology & Medicine. 2011;**30**:489-499

[22] Berliner LJ. From spin-labeled proteins to *in vivo* EPR applications. European Biophysics Journal. 2010;**39**:579-588

[23] Mason RP. Using anti-5,5-dimethyl-1-pyrroline N-oxide (anti-DMPO) to detect protein radicals in time and space with immuno-spin trapping. Free Radical Biology & Medicine. 2004;**36**:1214-1223

[24] Ramirez DC, Mason RP. Immuno-spin trapping: Detection of protein-centered radicals. Current Protocols in Toxicology. 2005;**17**:17

[25] Gomez-Mejiba SE, Zhai Z, Akram H, Deterding LJ, Hensley K, Smith N, Towner RA, Tomer KB, Mason RP, Ramirez DC. Immuno-spin trapping of protein and DNA radicals: "Tagging" free radicals to locate and understand the redox process. Free Radical Biology & Medicine. 2009;**46**:853-865

[26] Khoo NK, Cantu-Medellin N, St Croix C, Kelley EE. *In vivo* immuno-spin trapping: Imaging the footprints of oxidative stress. Current Protocols in Cytometry. 2015;**74**: 12.42.1-12.4211

[27] Mason RP. Imaging free radicals in organelles, cells, tissue, and *in vivo* with immuno-spin trapping. Redox Biology. 2016;**8**:422-429

[28] Gomez-Mejiba SE, Zhai Z, Della-Vedova MC, Muñoz MD, Chatterjee S, Towner RA, Hensley K, Floyd RA, Mason RP, Ramirez DC. Immuno-spin trapping from biochemistry

to medicine: Advances, challenges, and pitfalls. Focus on protein-centered radicals. Biochimica et Biophysica Acta. 2014;**1840**(2):722-729

[29] Towner RA, Smith N, Saunders D, Henderson M, Downum K, Lupu F, Silasi-Mansat R, Ramirez DC, Gomez-Mejiba SE, Bonini MG, Ehrenshaft M, Mason RP. *In vivo* imaging of immuno-spin trapped radicals with molecular MRI in a mouse diabetes model. Diabetes. 2012;**61**:2405-2413

[30] Towner RA, Smith N, Saunders D, Carrizales J, Lupu F, Silasi-Mansat R, Ehrenshaft M, Mason RP. *In vivo* targeted molecular magnetic resonance imaging of free radicals in diabetic cardiomyopathy within mice. Free Radical Research. 2015;**49**:1140-1146

[31] Towner RA, Garteiser P, Bozza F, Smith N, Saunders D, d'Avila JCP, Magno F, Oliveira MF, Ehrenshaft M, Lupu F, Silasi-Mansat R, Ramirez DC, Gomez-Mejiba SE, Mason RP, Faria-Neto HCC. *In vivo* detection of free radicals in mouse septic encephalopathy using molecular MRI and immuno-spin-trapping. Free Radical Biology & Medicine. 2013;**65**:828-837

[32] Towner RA, Smith N, Saunders D, Lupu F, Silasi-Mansat R, West M, Ramirez DC, Gomez-Mejiba SE, Bonini MG, Mason RP, Ehrenshaft M, Hensley K. *In vivo* detection of free radicals using molecular MRI and immuno-spin-trapping in a mouse model for amyotrophic lateral sclerosis (ALS). Free Radical Biology and Medicine. 2013;**63**:351-360

[33] Towner RA, Smith N, Saunders D, De Souza PC, Henry L, Lupu F, Silasi-Mansat R, Ehrenshaft M, Mason RP, Gomez-Mejiba SE, Ramirez DC. Combined molecular MRI and immuno-spin-trapping for *in vivo* detection of free radicals in orthotopic mouse GL261 gliomas. Biochimica et Biophysica Acta. 2013;**1832**:2153-2161

[34] Coutinho de Souza P, Smith N, Atolagbe O, Ziegler J, Nijoku C, Lerner M, Ehrenshaft M, Mason RP, Meek B, Plafker SM, Saunders D, Mamedova N, Towner RA. OKN-007 decreases free radicals levels in a preclinical F98 rat glioma model. Free Radical Biology & Medicine. 2015;**87**:157-168

[35] Ribou AC. Synthetic sensors for reactive oxygen species detection and quantification: A critical review of current methods. Antioxidants & Redox Signaling. 2016;**25**:520-533

[36] Bonini MG, Rota C, Tomasi A, Mason RP. The oxidation of 2′,7′-dichorofluorescin to reactive oxygen species: A self-fulfilling prophesy? Free Radical Biology & Medicine. 2006;**40**:968-975

[37] Liu F, Du J, Song D, Xu M, Sun G. A sensitive fluorescent sensor for the detection of endogenous hydroxyl radicals in living cells and bacteria and direct imaging with respect to its ecotoxicity in living zebra fish. Chemical Communications. 2016;**52**:4636-4639

[38] Hu JJ, Wong NK, Ye S, Chen X, Lu MY, Zhao AQ, Guo Y, Ma AC, Leung AY, Shen J, Yang D. Fluorescent probe HKSOX-1 for imaging and detection of endogenous superoxide in live cells and *in vivo*. Journal of the American Chemical Society. 2015;**137**:6837-6843

[39] Liu X, Liu S, Liang G. Fluorescence turn-on for the highly selective detection of nitric oxide *in vitro* and in living cells. Analyst. 2016;**141**:2600-2605

[40] Gupta N, Reja SI, Bhalla V, Gupta M, Kaur G, Kumar M. An approach for the selective detection of nitric oxide in biological systems: An *in vitro* and *in vivo* perspective. Chemistry, an Asian Journal. 2016;**11**:1020-1027

[41] Iverson NM, Strano MS, Wogan GN. *In vivo* delivery of nitric oxide-sensing, single-walled carbon nanotubes. Current Protocols in Chemical Biology. 2015;**7**:93-102

[42] Li Z, Liang T, Lv S, Zhuang Q, Liu Z. A rationally designed upconversion nanoprobe for *in vivo* detection of hydroxyl radical. Journal of the American Chemical Society. 2015;**137**:11179-11185

[43] Huang Y, Yu F, Wang J, Chen L. Near-infrared fluorescence probe for *in situ* detection of superoxide anion and hydrogen polysulfides in mitochondrial oxidative stress. Analytical Chemistry. 2016;**88**:4122-4129

[44] Zhang J, Li C, Zhang R, Zhang F, Liu W, Liu X, Le SM-Y, Zhang H. A phosphinate-based near-infrared fluorescence probe for imaging the superoxide radical anion *in vitro* and *in vivo*. Chemical Communications. 2016;**52**:2679-2682

[45] Iverson NM, Barone PW, Shandell M, Trudel LJ, Sen S, Sen F, Ivanov V, Atolia E, Farias E, McNicholas TP, Reuel N, Parry NM, Wogan GN, Strano MS. *In vivo* biosensing via tissue-localizable near-infrared-fluorecent single-walled carbon nanotubes. Nature Nanotechnology. 2013;**8**:873-880

[46] Shvedova AA, Kisin ER, Murray AR, Mouithys-Mickalad A, Stadler K, Mason RP, Kadiiska M. ESR evidence for *in vivo* formation of free radicals in tissue of mice exposed to single-walled carbon nanotubes. Free Radical Biology & Medicine. 2014;**73**:154-165

[47] Rayner CL, Gole GA, Bottle SE, Barnett NL. Dynamic, *in vivo*, real-time detection of retinal oxidative status in a model of elevated intraocular pressure using a novel, reversibly responsive, profluorescent nitroxide probe. Experimental Eye Research. 2014;**129**:48-56

[48] Du L, Huang S, Zhuang Q, Jia H, Rockenbauer A, Liu Y, Liu KJ, Liu Y. Highly sensitive free radical detection by nitrone-functionalized gold nanoparticles. Nanoscale. 2014; **6**:1646-1652

[49] Berkowitz BA, Lewin AS, Biswal MR, Bredell BX, Davis C, Roberts R. MRI of retinal free radical production with laminar resolution in vivo. Investigative Ophthalmology & Visual Science. 2016;**57**:577-585

[50] Berkowitz BA, Lenning J, Khetarpal N, Tran C, Wu JY, Berri AM, Dernay K, Haacke EM, Shafie-Khorassani F, Podolsky RH, Gant JC, Maimaiti S, Thibault O, Murphy GG, Bennett BM, Roberts R. In vivo imaging of prodromal hippocampus CA1 subfield oxidative stress in models of Alzheimer disease and Angelman syndrome. The FASEB Journal. 2017. Epub ahead of print. DOI: 10.1096/fj.201700229R

[51] Tain RW, Scotti AM, Li W, Zhou XJ, Cai K. Imaging short-lived reactive oxygen species (ROS) with endogenous contrast MRI. Journal of Magnetic Resonance Imaging. 2017. Epub ahead of print. DOI: 10.1002/jmri.25763

[52] Jerome NP, Papoutsaki MV, Orton MR, Parkes HG, Winfield JM, Boss MA, Leach MO, deSouza NM, Collins DJ. Development of a temperature-controlled phantom for magnetic resonance quality assurance of diffusion, dynamic, and relaxometry measurements. Medical Physics. 2016;**43**:2998

[53] Spear JT, Gore JC. New insights into rotating frame relaxation at high field. NMR in Biomedicine. 2016;**29**:1258-1273

[54] Eto H, Hyodo F, Kosem N, Kobayashi R, Yasukawa K, Nakao M, Kiniwa M, Utsumi H. Redox imaging of skeletal muscle using in vivo DNP-MRI and its application to an animal model of local inflammation. Free Radical Biology & Medicine. 2015;**89**:1097-1104

[55] Janzen EG, Towner RA. Aminoxyl radicals as MRI contrast agents. In: Zhdanov R, editor. Bioactive Spin Labels. Berlin: Springer-Verlag; 1992. pp. 573-583

[56] Hyodo F, Ito S, Eto H, Nakaji T, Yasukawa K, Kobayashi R, Utsumi H. Development of redox metabolic imaging using endogenous molecules. Yakugaku Zasshi. 2016; **136**:1107-1114

[57] Utsumi H, Hyodo F. Free radical imaging using in vivo dynamic nuclear polarization-MRI. Methods in Enzymology. 2015;**564**:553-571

[58] Ichikawa K, Yasukawa K. Imaging in vivo redox status in high spatial resolution with OMRI. Free Radical Research. 2012;**46**:1004-1010

[59] Yamamoto S, Watabe T, Ikeda H, Ichikawa K, Nakao M, Kato K, Hatazawa J. Development of a PET/OMRI combined system for simultaneous imaging of positron and free radical probes for small animals. Medical Physics. 2016;**43**:5676